FLUCOME 2009
10th International Conference on Fluid Control, Measurements, and Visualization
August 17–21, 2009, Moscow, Russia

DEVELOPMENT OF A SEDIMENT DISCHARGE MEASUREMENT SYSTEM WITH ADCP

Atsuhiro, Yorozuya[1], Sachio Shintaku[2], Keizo Ejima[3], Kazuhiko Fukami[1], and Hirokatsu Kanazawa[2]

ABSTRACT

Authors developed a sediment discharge measurement system with ADCP. In terms of the sediment discharge measurement, the ADCP is powerful tools, since a bed-load velocity can be measured. At the same time, it has a disadvantage for estimating the velocity at vicinity of river bed, since ADCP has an unmesurable area around the river bed. In the mean time, authors realized that flow distribution around the river bed is indispensable for estimating the shear velocity, while other studies used entire velocity profile. Authors realized the importance and a contradiction, when we compared the estimated-shear velocity and the bed-load velocity. For solving the contradiction, the authors developed the algorism to 1) inter- and extrapolate velocity distribution, and 2) determined the shear velocity. For verified the authors' algorism, we conducted the experiment with an experimental flume in movable bed condition.

Keywords: development of bed-load measurement, estimation of shear velocity, ADCP, experimental study

INTRODUCTION

National institutes of Japan in hydraulics and hydrology with which the authors are affiliated have been engaged in the development of sediment-discharge measurement systems. Fixed-type systems have demonstrated their functions successfully. At the same time, they have shown some serious disadvantages, such as susceptibility to site conditions, immobility, and high cost. Mobile-type sediment samplers were widely used nationwide about 40 years ago to measure bed-load discharge. However, observed results, especially those during large-scale flooding, were not accepted as appropriate (Yamamoto and Nishio, 1991), assumingly because of the landing condition of a sampler on a river bed or the heterogeneity of a river-bed form. In fact, field engineers have experienced different bed-load discharges by three or four orders of magnitude under the similar hydraulic conditions. To obtain reliable representative values, the authors have focused attention on bed-load velocity in a velocity field around an area of interest, instead of that at a certain point, which can be obtained by an Acoustic Doppler

[1] International Centre for Water Hazard and Risk Management (ICHARM) under the auspices of UNESCO, Public Works Research Institute (PWRI), e-mail: yorozuya@pwri.go.jp
[2] National Institute for Land and Infrastructure Management, Ministry of Land, Infrastructure and Transport and Tourism, Japan, email: shintaku-c92ta@nilim.go.jp
[3] Pacific Consultants Co., LTD., email: keizou.ejima@ss.pacific.co.jp

Current Profiler (ADCP). Once a bed-load velocity is observed, the sediment discharge can be estimated with the depth of the bed-load layer, which is a function of shear stress. Therefore, for completing the ADCP system for more reliable measurement, more accurate estimation of shear stress is indispensable. Moreover, since ADCP can measure both vertical velocity profiles and bed-load velocities, it is possible to use ADCP in a bed-load measurement system as Rennie (2002) proposed. In this paper, the authors will discuss 1) methods to estimate shear stress from vertical velocity distribution from ADCP, 2) comparison of the newly developed equation, conventional bed load ones, and observed bed-load discharges from an experimental flume, and finally 3) application of the ADCP system to field measurement during flooding.

In this study, the authors conducted an experimental study using an experimental flume in movable-bed conditions to verify the developed algorithm. Also, the bed-load discharge measurements and estimations were compared. The experimental results showed the sediment discharges obtained by using the newly developed ADCP system had good agreement with those of the conventional equations, as well as observed bed loads by a sediment sampler.

METHOD

The authors employed an experimental flume (4 m wide, 1 m deep, 80 m long) with a mobile bed condition. The test section (15 m long) was selected starting at 65 m from the inlet. Bed-load transport experiments using sand with a uniform size of 3 mm were conducted at water discharges of 1.75, 2.5, and 3.5 m^3/s, which resulted in non-dimensional shear stresses of 0.07, 0.08, and 0.19. Initially, a flat bed with a 30 cm sand layer and a water depth of 60 cm was maintained.

A 2.0 MHz StreamPro ADCP manufactured by RD instruments was employed for measuring bed-loads and water velocity distributions. The StreamPro ADCP has 4 beams mounted at 20 degree angles. Measurement accuracy is $\pm$1.0%, or $\pm$0.2 cm/s. It originally outputs measured values at an interval of 1 second. In the experiments, the ADCP was submerged about 15 cm from the initial water surface and had an immeasurable area of 10 cm. Therefore, the device was capable of measuring about 8 layers of vertical flow distribution with a cell size of 3 cm.

To measure flow properties, an experimental carrier was mounted with the StreamPro ADCP, 6 capacitance-type wave gauges at an interval of 0.5 m in the longitudinal direction at the center of the flume, and 2 wave gauges in the cross sectional direction. The flow properties in every 5 m length of the 15 m test section were obtained in an 6-minute observation; then, the carrier moved downstream to conduct other two sets of measurement. Since it was practically impossible to keep the flow consistent, an energy slope was used for obtaining the averaged shear stress at the river bed.

Also, bed-load discharges were measured with a TR-2 sediment sampler fabricated by the United States Geological Survey (USGS) during the experiments. The sampling was conducted more than 5 times and then averaged for representative values. Finally, bathymetry was measured to obtain the bed form after water was drained from the experimental flume.

ESTIMATION OF SHEAR VELOCITY

To estimate shear velocities based on ADCP–collected data, log-law with the entire data set is usually applied (Rennie, 2002; Sime et al, 2007). The equation is as follows;

$$u(z) = \frac{u_*}{\kappa}\ln(z) + \frac{u_*}{\kappa}\ln\left(\frac{30}{k_s}\right) \tag{1}$$

where $u(z)$ is the velocity at the point of z, z is the vertical elevation from the river bed, κ is the von

Karman constant, which is about 0.4, k_s is the bed roughness. To obtain the values of the shear velocity in Eq. (1), several different methods can be considered. The authors selected curve fitting with natural log for determining a and b in the equation of $u(z) = a\ln(z) + b$.

On the other hand, Nakagawa et al. (1981) estimated shear velocities over both smooth and rough stripe beds. They separated the zones into inner and outer zones, and estimated the shear velocity in the inner zone using log-law, instead of the entire velocity profile. Regarding the velocity profile associated with the bed shape, Yalin (1977) hypothesized that a flow distribution, which was relatively faster around the river bed and slower around the water surface, could be computed as lower shear stress based on Eq.1 using the entire velocity profile, and suggested possible erosion in the river bed under such a condition. Since bed degradation should be correlated to the estimated shear velocity, the shear stress cannot be estimated using the entire velocity profile. Therefore, based on the knowledge from Nakagawa and Yalin, the authors developed an algorism to estimate shear velocities from ADCP-collected data as explained in the following paragraph. Additionally, the authors tried to develop an algorism based on un-averaged data sets, since physics in the experimental flume with a higher shear stress is a highly unsteady condition.

To develop the algorism, the authors first smoothed a longitudinal velocity profile by using noisy ADCP raw data. Several different smoothing techniques were considered, such as the best fit curve with Eq.1, moving average, and the Fourier series expansion, which the authors selected. Prior to smoothing the profile, it was necessary to extrapolate the velocity distribution in both top and bottom immeasurable zones. Muste (2007) mentioned that extrapolation of power law could be applied to the top and bottom immeasurable zones. Regarding the estimation of the shear stress, the bottom immeasurable zone needed to be estimated with careful consideration. In general, when ADCP measures velocities in a retarding area, inflection points should appear. In such a case, it is desirable that the velocity distribution has a convex or concave in measurable and bottom-immeasurable areas, instead of two different convex curves. The algorism developed by the authors required several steps to complete the profile smoothing: 1) a curve fitting was conducted with Eq.1 in the measured area and the shear velocity u_{*1} was calculated, 2) another curve fitting was conducted with Eq.1 with one value at the lowest point and almost zero values at the near river-bed area (e.g. u = 0.01 cm/s at z = 0.01 m) and the shear velocity u_{*2} was calculated, 3) a concave curve was applied to the bottom zone if u_{*1} is larger than u_{*2}, while a convex curve if u_{*1} is smaller than u_{*2}, and 4) the applied curve was smoothed using Eq.(2) below.

$$u(z) = \sum_{k=1}^{k_{\mathrm{mode}}} u_{kc} \cos\left(\frac{\pi(k-1)z}{h}\right) + \sum_{k=1}^{k_{\mathrm{mode}}} u_{ks} \sin\left(\frac{\pi(k-1)z}{h}\right) \quad (2).$$

where u_{kc} and u_{ks} are coefficients in each k which can be determined as square of a deviation; $[u(z) - u_{ob}(z)]^2$ makes the minimum value. Here $u_{ob}(z)$ is the velocity obtained by ADCP, including the extrapolated values in the top and bottom unmeasurable zones. When k_{mode} is infinity, u(z) is exactly the same as $u_{ob}(z)$ which produces zigzag curves; therefore, the determination of appropriate k_{mode} is indispensable for obtaining smooth curves. Incidentally, ADCP had error velocities, which indicates the quality of observed values. For example, when a flow field is uniform in the measurement area, the error velocity is zero, which indicates that the deviation is also zero. Conversely, when the error velocity shows some values, the deviation can show a value of the corresponding magnitude. To incorporate this relationship between the error velocity and the deviation in the algorism, 5) the authors made judgments on value k based on the relationship. When the error velocity was larger than the deviation, k increased, while if the opposite is the case, k determined. The determination of value k made it possible to draw velocity distributions. 6) To determine the shear velocity, the inner zone, which was similar to the one in Nakagawa (1981), was employed, to estimate the shear velocity using Eq. (1) and velocity profile from the bottom to the location where velocity has the first local maximum. On the other hand, 7) when a concave curve was applied in the third step of the algorism, the shear velocity was set to match the bed-load velocity. Authors applied the idea based on figures in Egashira and Ashida (1972). These seven steps completed the authors' algorism. Regarding the verification of the estimated shear-velocity, comparing it with the bed-load velocity was valid, since the shear velocity represents external forces acting on the river bed, while the bed-load velocity is the consequence of their action. Therefore, the authors reasonably assumed that two velocities should have a positive correlation. The authors will later discuss this correlation for verification purposes.

RESULTS OF ESTIMATION OF SHEAR STRESS

Fig.1 shows one of the experimental results with the condition of $\tau_* = 0.3$. It shows the time series of a stream-wise velocity distribution taken by ADCP expressed in different contour colors. The water surface obtained by the wave gauges located in the vicinity of ADCP is a blue curve, and a bathymetry taken by ADCP in a black curve. For the purposes of eliminating missing data, ADCP was installed at the depth of 0.743 m. The area between 0.7 m and the blue curve is the unmeasured area. During the experiments, the peak of the sand wave came at 200 seconds, while the water surface varies. The experiments resulted in several different flow profiles, such as flows at the top and bottom of the crest.

Fig.2 shows the shear velocities estimated by the authors' algorism (u_*-authors) and Eq.1 (u_*-Eq.1), the bed-load velocity, the water surface variation, and the river-bed elevation on the right vertical axis. 10-time moving averages were applied to those data. Both shear velocities show very differently, especially at the crest and base of the sand wave. For example, when the time is around 120 seconds, which represents the flow around the base, u_*-Eq.1 is much larger than u_*-authors, while the bed-load velocity exhibits the similar magnitude to that by u_*-authors. Likewise, when the time is around 200 and 330 seconds, which represents the flow at the crest, they show an opposite trend. Overall, u_*-authors has a positive correlation with the bed-load velocity, even though there are some limitations, as seen in the case where the time is 220 seconds. For further discussion, longitudinal velocity profiles at different locations were drawn in Fig.3 (a) and (b).

Fig.3 (a) and (b) show the longitudinal distributions of the stream-wise velocity (u-observed), the vertical velocity (w), the error velocity (dw), the velocity curve-fitted by Eq.1 (u-Eq.1), and the velocity fitted by the authors' algorism (u-authors). Fig.3 (a) is a profile obtained at 120 seconds in the Fig.1, which represents a profile around the base of the sand wave. Fig.3 (b) is a profile at 200 seconds, which represents one at the crest. As shown in Fig.3, both u-Eq.1 and u-authors are nicely interpolated with u-observed. In addition, differences between interpolated and observed values have the similar magnitude of dw, which is exactly the authors' intension as explained in the previous section. To validate the estimation of the shear velocity, Table 1 and Figs.3 are needed to be discussed. The authors' algorism indicates that the flow distribution of Fig.3(a) around the river bed is a concave curve; therefore, u_*-authors is smaller than u_*-Eq.1, while the bed-load velocity has the same magnitude as u_*-authors. On the other hand, u-observed in Fig.3(b) shows a negative gradient; therefore, u_*-Eq.1 indicates a negative value. However, u_*-authors shows 0.27 m/s, while the bed-load velocity shows 0.45 m/s. Based on the discussion, the authors verified our method at two representative points. In the following chapter, authors explained overall relationship between the bed-load velocity and the shear velocity.

Fig.4 shows the relationship between the shear velocity and the bed-load velocity after taking a moving average of 10 seconds. Observed values from the 9 experiments were used for blue dots. Red dots in each figure indicate averaged values in every 0.5 cm/s of the shear velocity. Fig.4 (a) shows the authors' algorism about the shear velocity, while Fig.4 (b) shows u_* by Eq.1. As Fig.4 (a) indicates, there are two areas with different bed-load velocities of less than 2 cm/s and more than 2 cm/s. The first area indicates that the river bed does not move sometimes, even when the shear velocity is higher than the level at which it is supposed to move. Some other physical processes might need to be considered. The second area indicates an increase in shear velocity as the bed-load velocity increases, as the authors expected. Regarding the distribution of the red dots, the authors draw a black line to clearly show our intension. The black line starts from the 8 cm/s point at 45 degrees, which can be explained using the following mathematical expression:

$$bedload \quad velocity = f\left(u_{*-authors} - u_{*c}\right) \tag{3}$$

In the case of Fig. 4 (a), the authors could use the linear function with the slope of 1, and u_{*c} of 8 cm/s for this *f*( ). This trend is similar to the relation derived by Ashida and Michiue (1972), which justifies the authors' method. On the other hand, the distribution of Fig.4 (b) shows a negative correlation, over all, which is very different.

As a summary of this section, the authors can reasonably conclude that u_*-authors has a positive correlation with the bed-load velocity, and that the algorism developed by the authors is a better estimator compared with Eq.1.

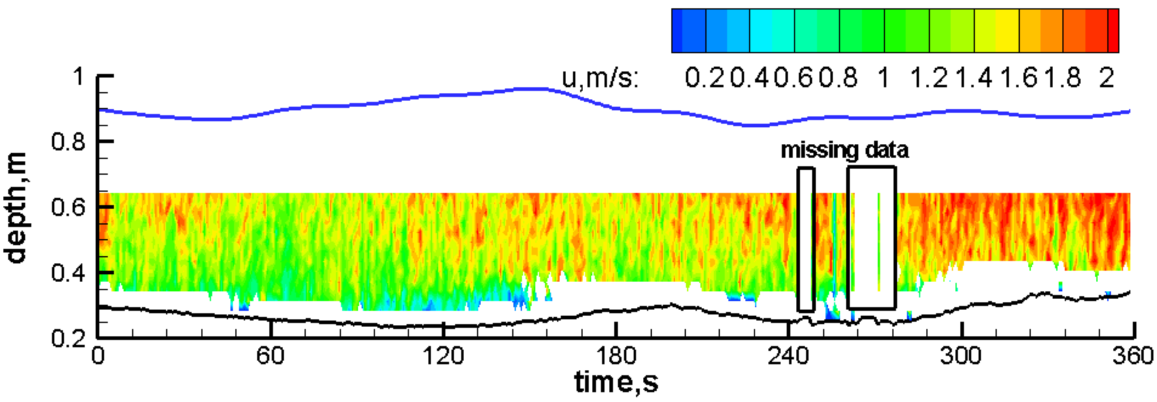

Fig. 1. Time series of velocity profile in contour, water surface, and river bed

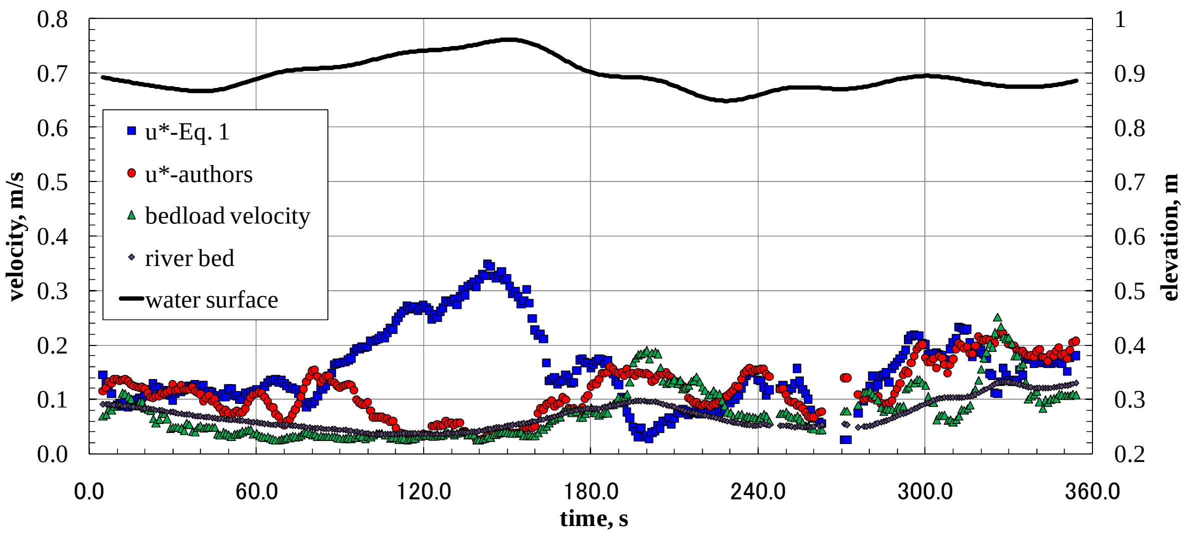

Fig. 2. Time series of shear velocities, bed-load velocity, water surface, and river bed

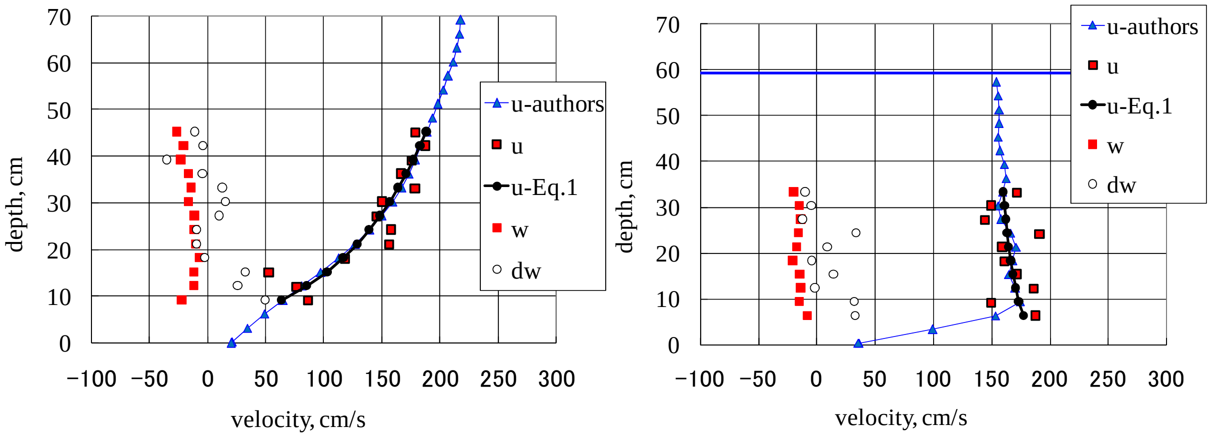

(a) flow field around base at 120 s **(b) flow field at crest at 200 s**

Fig. 3. Velocity distribution when $\tau_* = 0.3$

Table 1. Comparison of shear velocity

Time, s	Figure	Bed-load velocity, m/s	u_*-Eq.1, m/s	u_*-authors, m/s
120	Fig.3 (a)	0.04	0.21	0.03
200	Fig.3 (b)	0.45	-0.04	0.27

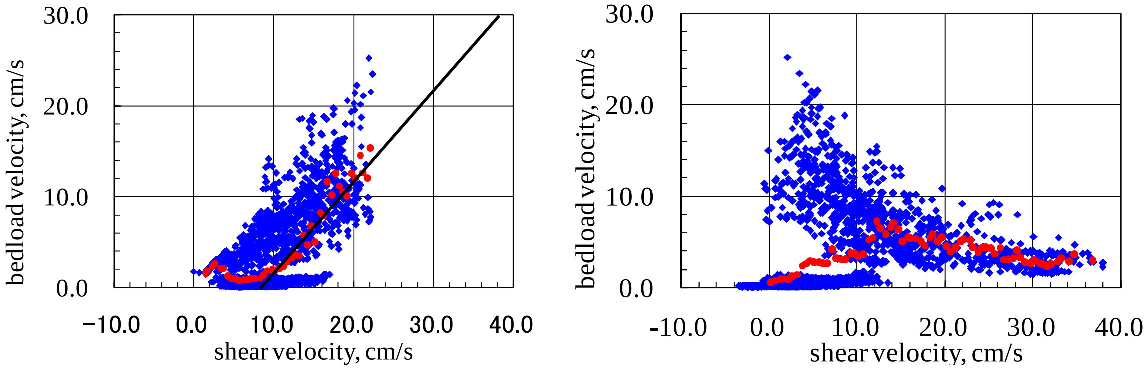

(a) Estimated by authors' algorism **(b) Estimated by Eq.1**

Fig. 4. Relation between shear velocity and bed-load velocity

ESTIMATION OF BED-LOAD TRANPORT

To estimate the bed-load transport rate, van Rijn (1984) introduced the equation as

$$q_B = f\left(C, u_b, h_s\right) \qquad (4).$$

Here, q_B is bed-load transport rate, u_b is bed-load velocity, C is concentration of sediment, and h_s is depth of bed-load layer. Same concept with Eq.(4), Egashira and Ashida (1992), Ramooz and Rennie (2007), and others use following equation;

$$q_B = \overline{v_s} \cdot h_s \cdot \overline{c_s} \quad (5).$$

Here, $\overline{v_s}$ is the average velocity of bed-load layer, and $\overline{c_s}$ is averaged sediment concentration, which is $c_w/2$,where c_w is sediment concentration at bottom; c_w = 0.6. Since authors measure the bed-load velocity with ADCP, we could apply the bed-load velocity to the $\overline{v_s}$. Also Egashira and Ashida (1972) derived the equation about h_s, such as

$$\frac{h_s}{d} = \frac{2}{c_w \cdot \cos\theta \cdot \{\tan\phi_s/(1+\alpha) - \tan\theta\}} \tau_* \quad (6)$$

Here, d is sediment diameter, ϕ_s is internal friction angle, which is 38.5 degree, θ is local slope of river bed, and τ_* is non-dimensional shear stress. ADCP measures river bed with four different beams. Usually, 3rd beam and 4th beam look upstream and downstream. In this paper, the authors use only two beam for determining the local slope, since direction of flow predominated. For the purpose of field measurement, it might be better to use four different beams. As discussed before in the Eq. (4) and (5), those equations have advantage to be applied in this measurement system, since most of the sediment/water flow properties can be measured by ADCP. Though, h_s need to be determined from empirical equation, $\overline{v_s}$ is measured value. Certainly, as the number of estimated parameter is less, the measurement system is more reliable; therefore, the authors' measurement system is powerful. In addition, in the case when the bed-load velocity cannot be measured due to difficult observing conditions, empirical equation such as Eq. (3) can be applied as well. Following paragraph shows one of the experimental results related to the bed-load transport rate. As conclusion of the estimation method, authors applied Eq.(4) as basis of the estimation equation, with 1) employing observed bed-load velocity, 2) applying Eq.(6), and 3) applying the authors algorism for estimating the shear velocity. Next paragraph explains about one of the experimental results.

Fig. 5 shows the time series of the bed-load transport rate; bed-load, non-dimensional flow depth of sediment layer; h_s/d, shear velocity by authors methods; u_*-authors, the bed-load velocity, water surface elevation and river bed. Horizontal axis is time in second, vertical axis of the right side is bed load; qs divided by 1,000 in m^2/s, velocity in m/s including the bed-load/shear velocity, and elevation in m including water surface and river bed. Vertical axis of the left side is h_s/d in non-dimensional unit. As seen in this figure, relationship between the bed-load transport rate and each term are depicted in the figure. As already discussed before with Fig.2, u_*-authors and the bed-load velocity are positively correlated each other. In addition, most of the other properties, as described in Eq.(4) and Eq.(5), should be positively correlated as well. Though, the trends is almost consistent in entire period, there are still some aspects needed to be mentioned.

For example, at 200 seconds, the relationship between the bed-load velocity, and bed load is strongly correlated each other, though maximum h_s/d appear at 210 seconds. On the other hand, at 225 seconds, the bed-load velocity starts to decreases with time, while the u_*-authors increases; consequently, the h_s/d and the bed-load increase. As other example, around 325 seconds, the bed-load velocity increase, while the u_*-authors does not increase that much; however, hs/d increases because local slope increases. At this time, the bed load has maximum number. As mentioned here, only measurement of the bed-load velocity does not work well, since other parameters affect strongly to the bed-load transport rate.

Other important aspect is that unsteadiness of the bed-load transportation rate. As this figure shows, the bed-load transportation rate varied with time from almost zero to more than 1×10^{-3} m^2/s. Actually, an average in between 100 and 160 seconds is 0.007×10^{-3} m^2/s, while the average in between 295 and 354 seconds is 0.40×10^{-3} m^2/s. Even though experimental condition such as water discharge and water-surface elevation at the downstream are kept constant, an unsteady result appears.

Table 2 shows comparison of the bed-load transport rate with both estimated by equation and collected by the sediment sampler. The bed-load transport rate in authors means that 1) estimating value in 360 seconds' experiments by authors' method, 2) taking average with 3 sets of measurements. For authors with Eq. (3) means that applying Eq.(3) with u_*-authors instead of observed bed-load velocity. Also average with 3 sets of measurement was taken, as well. Ashida and Michiue (1972), which is most commonly used in Japan, is applied for verification purposes. Finally, sediment sampler was employed. The values in the table show the result of 5 times sampling. Overall, three different estimator predicts the bed-load transport rate well. Though equation of Ashida and Michiue (1972) estimated slightly overly, if the order of magnitude is correct, then they are accepted as good estimator in general. If we could make close investigation, unsteady condition might be one of the reasons.

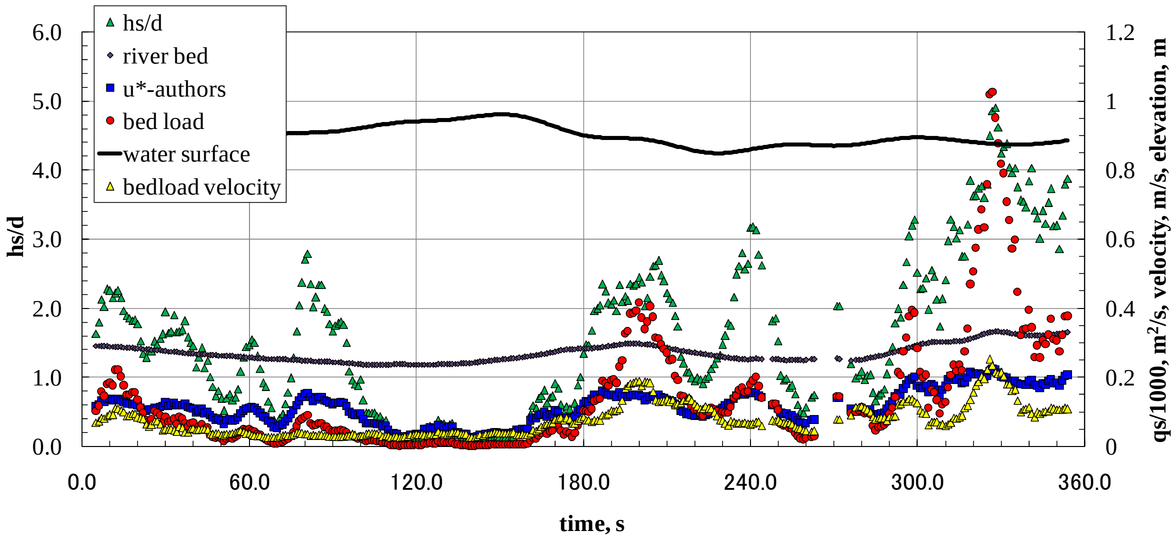

Fig. 5. Time series of bed-load transport rate, h_s/d, shear velocity, bed-load velocity, water surface elevation, and river bed.

Table 2. Comparison of bed-load transport rate

Water discharge, m^3/s	τ_*	Bed-load transport rate/1000., m^2/s			
		Authors	Authors with Eq.(3)	Ashida and Michiue (1972)	Sediment sampler
1.75	0.07	0.001	0.004	0.003	0.000
2.5	0.08	0.008	0.038	0.069	0.016
3.5	0.19	0.147	0.114	0.476	0.244

FURTHER STUDY AND CONCLUTION

The algorism for determining the shear velocity was developed by authors, and verified by the experimental study. Mainly, Fig. 4 represents our major contribution and success of the new developed algorism.

Regarding unsteady experimental condition as seen in Fig. 5, the authors have never regretted, or not considered this experiment as failure. Moreover, the authors sincerely accepted the result, since aims of the research is 1) not only a study for producing an equation for estimating the bed-load transport rate, 2) but also development of the bed-load measurement system in actual river. As a matter of fact, actual river condition cannot be maintained as uniform condition, even though water depth does not increase at a period of interests, as partially explained in the Fig.5. As mentioned in the introduction of the paper, field engineers have experienced very different sediment transport rate, even similar hydraulic condition. The authors assumed the landing condition is a major reason; however, the authors understood that unsteady sediment movement might be one of the important aspects, as well.

In the future, conducting the field measurement with similar setup is fundamental for further understanding of the sediment transport in actual river. It is worthy to mention that same setup can be used to conduct a field measurement even in unsteady condition. Actually, the field measurements with ADCP mounted on un-manned boats have been conducted and successfully by authors. Accumulation of measured values enriches the discussion.

ACKNOWLEDGMENTS

The authors would like to thank Dr. Osti Rabindra for discussing with us about the sediment transport equation. Also the authors would like to thank Mr. Yoshiki Shiraishi for discussing with us about the inter-/extrapolation of flow field.

REFERENCES

Ashida, M. and Michiue, M. (1972), “Study on hydraulic resistance and bed-load transport rate in alluvial streams,” Proc. Japan Society of Civil Engineers JSCE 206, 59-69 (in Japanese).

Egashira S. and Ashida K. (1992), “Unified view of the mechanics of debris flow and bed load,” Shen H. H. et al. (eds.), Advances in Micromechanics of Granular Materials, Elsevier, 391-400.

Nakagawa, H., I.Neau & A. Tominaga (1981), “Turbulent structure with and without cellular secondary currents over various bed conditions,” Annuals, Disaster Prevention Research Institute, Kyoto University, 24B: 315-338 (in Japanese).

Ramooz, R., and Rennie, C. (2007), “Laboratory ADCP Bedload Measurements: Comparison with Capture rates and Dune Tracking,” Hydraulic Measurements & Experimental Methods 2007 (ASCE/IAHR) Book of Extended Abstracts, Lake Placid, NY, pp.106-111.

Rennie and et al. (2002), “Measurement of bed load velocity using an Acoustic Doppler Current Profiler,” J. Hyd. Eng., Vol. 128, No. 5

Van Rijn, L. C., (1984) Sediment Tranport. Part I: bed load transport., Journal of Hydraulic Engineering, ASCE, v.110, no.10, p.1431-1456

Yalin (1977), Mechanics of sediment transport (2nd ed.), Pergamon press

Yamamoto and Nishio (1991), bed form, roughness, and sediment discharge on the river with larger sand and fine gravel, technical report of PWRI, No. 2944, ISSN 0386-5878